Improving MicroBooNE's Inclusive Single-Photon Search with Low-Energy Hadronic Identification

The MicroBooNE Collaboration*

June 22, 2026

Abstract

This analysis aims to further investigate MicroBooNE's inclusive single-photon search results [1], which reported a 2.2σ excess below 600 MeV in shower energy for events with no reconstructed protons using roughly half of MicroBooNE's dataset. Taken together with MiniBooNE's long-standing low-energy excess [2] and MicroBooNE's recent electron-like search results showing no observable excess with respect to Standard Model predictions [3], this result provides strong impetus for expanded exploration of the single-photon channel in Fermilab's short-baseline liquid-argon time projection chamber (LArTPC) experiments. By identifying and classifying isolated MeV-scale energy depositions, or blips, in the vicinity of single-photon events selected by the Wire-Cell reconstruction framework, we establish a more comprehensive labeling scheme for nearby hadronic content. In particular, blips found backwards along the shower axis indicate the presence of previously-unidentified final-state protons, while elevated blip counts at wide angles signal the presence of final-state neutrons. By applying this new technique to its full dataset, MicroBooNE will perform a purer and higher-statistics test of the truly isolated nature of its modest photon-like excess, furthering its hunt for the presence of unexpected new physics beyond the Standard Model. This public note documents the current status of this enhanced single-photon analysis from MicroBooNE, which will form a major piece of the collaboration's final generation of low-energy-excess-oriented MicroBooNE results.

1 Introduction

By applying the existing Wire-Cell-based, BDT-enhanced (Boosted Decision Tree) selection chain to MicroBooNE's full dataset, the inclusive single-photon sample will be roughly doubled in size compared to [1]. With this enlarged dataset, the new and more comprehensive hadronic characterization scheme developed in this work, leveraging blip-based proton and neutron identification, can be applied to provide a finer decomposition of the selected events into exclusive final-state categories. This will allow us to assess whether any remaining excess is concentrated in a specific region of hadronic phase space or is broadly distributed, which in turn will shed light on whether the excess is consistent with systematic effects, or a signal of physics beyond the Standard Model.

1.1 Motivation

MicroBooNE, built to investigate the long-standing MiniBooNE low-energy excess (LEE) [2] anomaly as part of its physics program, pursued a broad program of LEE searches across both

*Email: microboone_info@fnal.gov

electron-like and photon-like channels. The electron-like search disfavored both a purely electron-neutrino interpretation and the 3+1 light sterile neutrino hypothesis as explanations for the MiniBooNE excess [3, 4]. Similarly, the exclusive photon-like results — including an enhanced neutral current (NC) Δ production measurement [5], coherent single-photon production [6], and the first test of a dark-sector interpretation via e^+e^- pairs [7] — found no observable excess consistent with the LEE. Taken together, these null results, alongside a localized (2.2σ) excess in events with no reconstructed protons from the inclusive single-photon analysis [1], provide strong motivation for an expanded and more thorough exploration of the single-photon channel as a potential explanation for the MiniBooNE anomaly in short-baseline beam neutrino experiments.

Leveraging newly developed MeV-scale tools and techniques — namely, blip reconstruction [8] and electron-proton discrimination in the MeV-scale regime [9] — alongside additional selection criteria such as a cosmic ray veto intended to mitigate background events, we aim to further investigate the inclusive single-photon events by probing for distinguishing MeV-scale features. These may include low-energy hadronic activity in the form of blips arising from neutron multiple scattering, as well as low-energy protons below current reconstruction thresholds.

The potential value of blip-based cues in MicroBooNE's single photon events is illustrated in Figure 1 with four event displays from the inclusive single-photon data sample in Ref. [1]. The presence of a previously unidentified proton-like blip upstream from an "isolated" MicroBooNE photon-induced shower (top two images) would support the idea that the shower's true origin is a neutral-current ν-Ar interaction. A similar conclusion could also be derived from the observation of a sizable population of electron-generated blips in a shower's vicinity (right two images), which indicates the presence of an inelastically-scattering final-state neutron. However, blip count consistent with ambient levels in the vicinity of a shower (bottom left) could signal that the shower originated in the decay of an invisible particle, a process that would not produce energetic final-state hadrons.

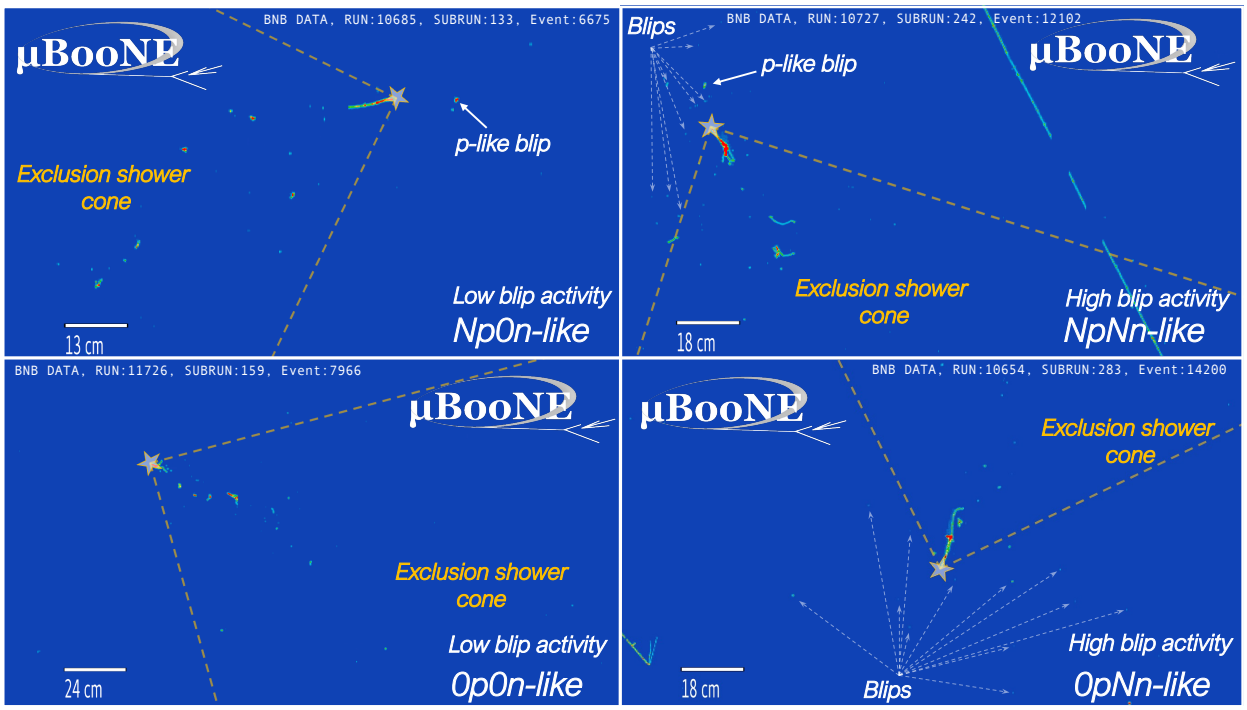

Figure 1: *Event displays of single shower events classified in terms of the exhibited blip activity into* ***Np0n-****,* ***NpNn-****,* ***0p0n-*** *and* ***0pNn-like*** *events. The star indicates the reconstructed shower vertex, origin of the exclusion "cone" region which encloses the shower and blip activity associated to it. Two characteristic blip types are visible: those with higher ionization density are proton-like, while the remainder are electron-like.*

2 Event selection and improvements

2.1 Signal event selection

The present analysis uses a small unblinded dataset (3.94×10^{19} POT), corresponding to roughly 3% of the total MicroBooNE data. We preserve the same signal definition as in the previous inclusive single-photon analysis for Runs 1–3 in Ref. [1] by applying the same BDT-based selection criteria to the present dataset in addition to a new Cosmic Ray Tagger (CRT) veto cut and Wire-Cell reconstructed proton proximity cut described below.

2.1.1 Changes to selection: CRT-veto cut

MicroBooNE's CRT system finished installation and commissioning in 2017, thus the CRT is available only in Runs 3–5. The implementation of a CRT veto cut in the updated inclusive single-photon analysis improves selection purity by rejecting events in which CRT hits are found in time with the beam window (1.6 μs). After applying the CRT-veto cut, signal events present an absolute reduction of 6.8%, however, the background categories cosmic data, Dirt/out of Fiducial Volume (FV) and charged current (CC) π^0 in FV, are reduced by 25.4%, 35.5% and 14.3% respectively, being the components mainly targeted by this cut in the event selection. These changes translate into a 2.3% purity increase of signal events with a simultaneous reduction in purity of 4.6% for the combined background cosmic data and Dirt/out of FV categories in the inclusive single-photon selection.

2.1.2 Changes to selection: Wire-Cell reconstructed proton proximity

Reconstructed protons are identified using Wire-Cell, which can reliably reconstruct protons with kinetic energies above 35 MeV. This threshold corresponds to a proton track of approximately 1 cm in length, spanning a few wire spacings, which represents the minimum range required to perform particle identification through reconstructed dE/dx measurements (energy deposited per unit length), and is comparable to the effective reconstruction threshold in Pandora, a multi-algorithm pattern recognition framework for LArTPC reconstruction. It is important to note that these proton criteria are entirely independent of the inclusive single-photon BDT, which does not incorporate any blip-related proton variables. While the distinction between zero-proton ($0p$) and multi-proton (Np) topologies was treated as a secondary consideration in the prior analysis, it has become a central focus of the present work, motivated by the outcome of that analysis. Accordingly, the proton multiplicity definition has been refined by additionally requiring that any reconstructed proton candidate lie within 75 cm of the reconstructed shower vertex. This proximity requirement ensures that only protons consistent with originating from the neutrino interaction vertex are counted, reducing contamination from secondary interactions or mis-reconstructed tracks unrelated to the primary interaction.

2.1.3 Updated inclusive single-photon event selection

Following the application of the baseline inclusive single-photon selection, the new CRT-veto requirement, and application of final-state proton multiplicity criteria, Figure 2 presents a first look at the inclusive single-photon events in terms of the number of protons reconstructed by Wire-Cell for the present dataset. The signal categories are identified within the stacked distributions by the magenta '1γ' component label. The displayed errors include only MC statistical uncertainties (hatched bands on the stacked colored histograms).

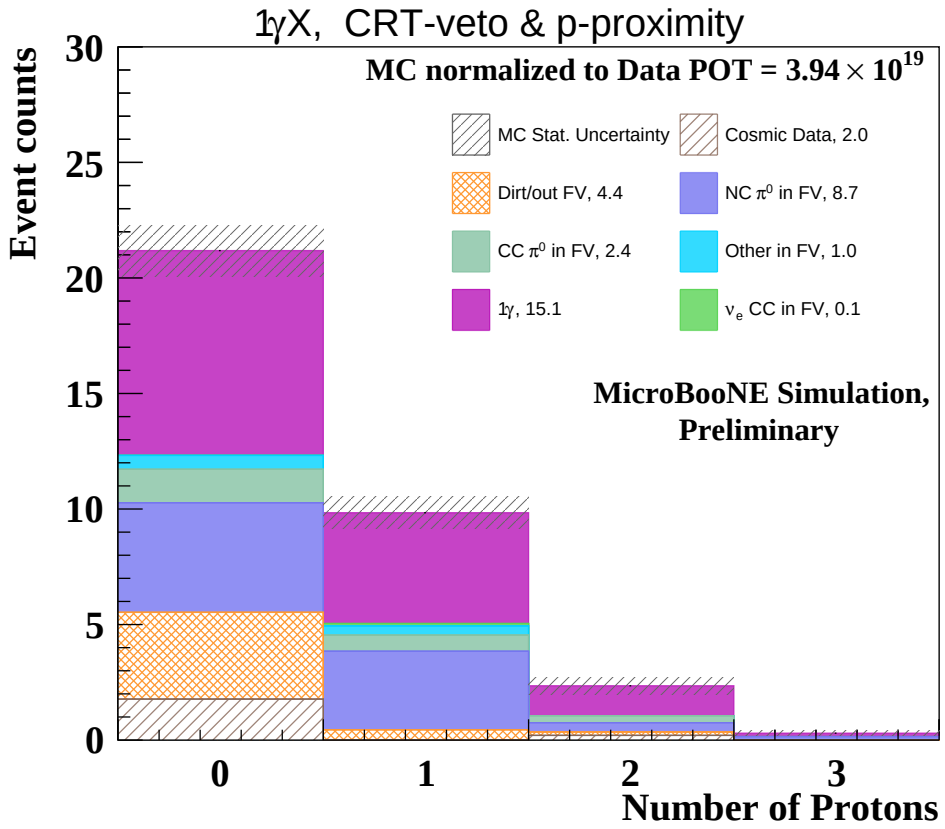

Figure 2: *Inclusive single-photon event selection with the addition of the CRT veto and the Wire-Cell proton vertex proximity cuts. Legend entries indicate the predicted number of events from signal and background categories after POT normalization.*

The dominant background contributions to the inclusive single-photon selection can be grouped into four categories, each presenting distinct but related challenges to the signal-background separation. Neutral-current interactions producing a π^0 (NC π^0) represent the most challenging background, since a π^0 decays into two photons, and events where one photon is missed or misclassified leave a single electromagnetic shower in the detector that is nearly indistinguishable from signal events. Charged-current muon neutrino interactions (ν_μ CC), with or without a π^0 in the final state, can mimic the signal topology when the muon track is either short or poorly reconstructed, making it difficult to distinguish from a photon-induced shower. Charged-current electron neutrino interactions (ν_e CC) introduce a genuine electron-induced shower into the final state, which closely resembles a photon shower in its calorimetric profile; the primary handles for separation in this case are the shower dE/dx at the start of the shower and the shower conversion distance, since photons, unlike electrons, do not deposit charge immediately at the interaction vertex. Finally, a residual category of backgrounds primarily encompasses cosmic-ray-induced events and neutrino interactions in which the true scattering vertex lies outside the TPC, but where the resulting ionizing particles travel into the fiducial volume and are reconstructed as a neutrino-like interaction contaminating the single-photon event selection.

3 MeV-Scale reconstruction in MicroBooNE

MicroBooNE has recently demonstrated exciting capabilities in the MeV energy regime. Through dedicated reconstruction efforts, the experiment has achieved the ability to identify and characterize low-energy signatures [8–11] at the MeV scale. This sensitivity provides a powerful tool that, in the context of the LEE searches, enables further investigations, most notably, the identification of low-energy hadronic activity as intended in this study.

3.1 Blip reconstruction

This analysis leverages blips, reconstructed isolated ionization depositions identified by BlipReco [8], a dedicated LArSoft toolkit. Further details on BlipReco are provided in Refs. [8, 9]. Reconstructed blip objects carry multiple attributes, including charge, energy, position (x, y, z), spatial extent along the drift direction and wire planes, and distance to the nearest track, from which additional secondary variables can be derived. The primary attributes used in this analysis are the blip energy and position, which, combined with neutrino interaction variables, allow us to define quantities of interest such as the distance from the blip to the shower vertex and the angle of the blip with respect to the shower direction. BlipReco also retrieves truth-level information, including the identity of the particle contributing the most energy to a given blip, enabling partial backtracking of the blip's true origins in MicroBooNE simulated events.

The analysis presented here is based on an unblinded sample of data, processed in MicroBooNE's most-recent data production campaign. This production is unique in its inclusion of BlipReco MeV-scale reconstructed objects alongside other high-level reconstructed variables, such as Wire-Cell inclusive single-shower BDT variables, Wire-Cell reconstructed proton variables, and reconstructed CRT information. To our knowledge, this represents the first-ever inclusion of MeV-scale reconstructed blip variables in a full-scale data production run for a LArTPC neutrino experiment. This inclusion ensures speedy generation of MeV-scale reconstructed variables for the complete MicroBooNE datasets, and enables implementation and consideration of blip-based analysis information into an updated inclusive single-photon analysis.

A consequence of the current data processing strategy is the continued use of standard region of interest (ROI) in the raw signal deconvolution and hit reconstruction settings during low-level processing, which propagates to the use of standard hit objects as input to all high-level shower, track, and blip reconstruction algorithms. While this ensures consistency with prior MicroBooNE physics analyses at the track and shower level, it results in a substantial pull-back in MeV-scale reconstruction capabilities compared to dedicated MicroBooNE MeV-scale analyses [8–10], which employed customized low-threshold ROI- and hit-finding settings applied to a more limited subset of beam-external data.

Thus, for this analysis, MicroBooNE achieves a volume-averaged blip reconstruction efficiency of 50% of its maximum value at 670 keV true electron energy; in contrast, prior lower-threshold blip analyses experienced a similar blip-finding threshold at 450 keV. Also in contrast to prior MicroBooNE MeV-scale analyses, our analysis will not take advantage of un-matched collection plane clusters reconstructed by BlipReco. While this choice further sacrifices performance at the lowest accessible blip energies (100–450 keV), it allows us to avoid increased background- and response-related uncertainties likely to be encountered in this regime. A more detailed description of the difference between low-threshold and standard-threshold blip reconstruction attributes are given in Ref. [8].

3.2 Signal blips

Since we are interested in characterizing blip activity in the vicinity of inclusive single-photon events, we define a fiducial volume around each shower vertex while excluding a conical region along the shower direction to avoid contamination from shower-related activity. Signal blips are defined by the following criteria:

1. Reconstructed in the active LArTPC volume.
2. Matched across at least 2 wire planes. This enhances the efficiency of low energy blips.
3. Component clusters cannot be adjacent to dead wires. This reduces blip contributions from mis-reconstructed tracks.

4. The closest 3D-distance to a long (>5 cm) track must be > 15 cm. This choice mitigates contributions from cosmic-induced blips, such as those from muon δ-ray radiative scatters.

5. A blip's 3D-distance, D, from the reconstructed shower vertex must be < 75 cm. This distance corresponds to multiple times the n/γ scattering length of $O(10$ cm). Thus, most of the blip activity from final-state hadrons near the shower would fall inside 75 cm, while nearly all ambient cosmic and radiogenic blip activity would occur outside it.

6. Not located within an exclusion region centered on the shower. The exclusion cone originates a from reconstructed shower vertex and is centered along the shower's reconstructed principal axis with an opening angle of $\beta = 90°$.

3.3 Indication of excess low-energy activity near single-photon events

As a first look at potential blip activity in inclusive single-photon events, we examined a filtered sample containing all inclusive single-photon event candidates in the BNB (Booster Neutrino Beam) data sample of Ref. [1], alongside a large sample of Run 3 unbiased beam-external (EXT) events collected via an external trigger in the absence of the neutrino beam, used in prior MeV-scale studies [8, 9]. The filtered BNB event sample was processed in a bespoke small-scale processing run with low-threshold reconstruction settings comparable to that of prior MeV-scale physics studies. For each BNB event, the blip selection criteria described above (with a looser radius of $R = 100$ cm) were applied with respect to the candidate single shower contained in that event. An identical selection was then also applied to a large number of events of the EXT dataset, assuming identical single shower attributes as the original BNB event, that is, vertices and their associated shower directions from signal inclusive single-shower BNB events are selected randomly and placed into EXT events to establish a reference for surveying the fiducial volume, providing a representative sample of ambient blips underlying the population of blips that truly accompany the single-shower BNB sample. After applying this selection on both datasets, EXT dataset results are then scaled downward according to the relative sizes of the BNB and EXT datasets.

Resulting signal blip distributions arising from these two datasets are presented in Figures 3a and 3b. In both of these plots, BNB candidates are separated into two categories: one event set designated as containing zero reconstructed protons according to the definitions of Ref. [1] and one designated as containing one or more reconstructed protons. These Figures show a clear excess of both signal blips and summed blip energies in the vicinity of single isolated showers. This observation clearly supports the hypothesis of additional sources of blip activity in the vicinity of the shower vertex beyond ambient radiogenics and cosmics. It is also interesting to note that blip multiplicities and total energies appear to be slightly higher for showers appearing in coincidence with reconstructed protons in the TPC.

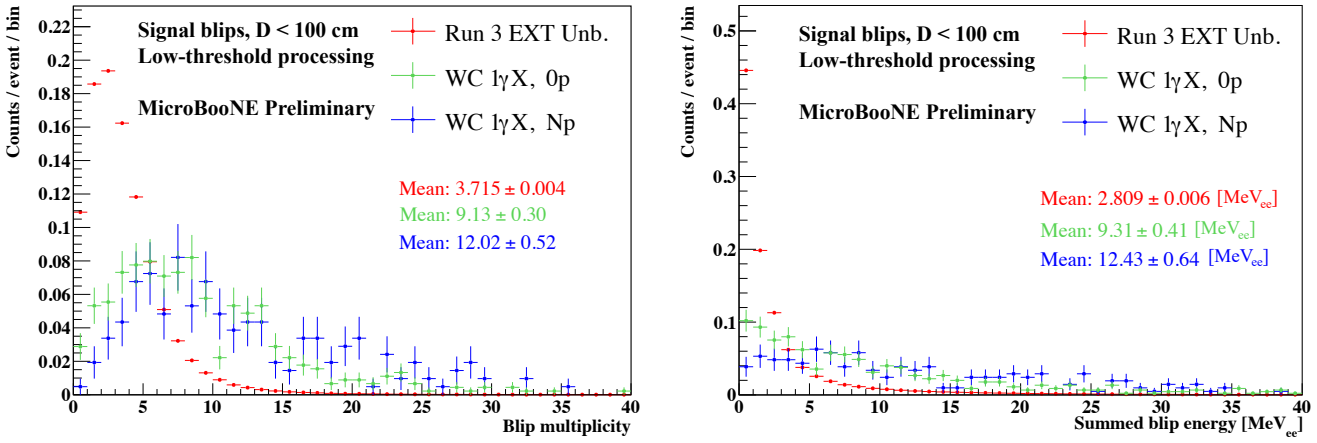

(a) Blip multiplicity distribution. *(b) Summed blip energy.*

Figure 3: *Blip multiplicity (left) and summed blip energy [MeV_{ee}] (right) for the Run 1–3 inclusive single-photon events ($1\gamma X$) with (Np) and without ($0p$) reconstructed protons samples compared to the EXT unbiased data with low-threshold processing. Both distributions indicate an excess of signal blip activity with respect to the baseline ambient radiogenic and cosmic blip activity in terms of blip multiplicity and summed energy. The blip energy is reported in electron-equivalent MeV, a scale calibrated to electron energy deposition.*

There are a few interesting potential sources of excess blips to consider. The first category is blips generated by de-excitation gamma rays emitted by the struck argon nucleus, which produce electron-like blips via Compton scattering. It is worth noting that de-excitation gammas are absent from our current simulation. In addition, neutrons produced in the neutrino interaction may undergo inelastic scattering, leaving behind electron-like blips — from gammas due to neutron capture on an argon nucleus — as well as proton-like blips when recoiling protons are knocked out of argon nuclei. While both electron-originating blip source categories have been previously described and observed in ArgoNeuT charged-current muon neutrino interactions [12], this is the first time that such an observation has been reported for an event set expected to be primarily composed of neutral-current neutrino interactions. To provide a more specific and conclusive investigation of these excess blips and their origins, we must perform a Monte Carlo (MC) simulation of the selected BNB event set and a dedicated data-MC comparison. However, this result augurs positively for the possibility of using MeV-scale reconstruction and blip-based variables to further purify a sample of truly isolated single-shower events.

4 Blip-based low-energy proton characterization

The identification of low-energy protons via blip-based reconstruction provides a powerful handle to enhance the $0p/Np$ classification of inclusive single-photon events, recovering hadronic activity that would otherwise fall below the threshold of standard tracking algorithms. With blips, we aim to identify low-energy protons from the actual neutrino interaction vertex that may be overlooked by standard reconstruction tools. For this purpose, we define backtracking regions with respect to the shower vertex and direction, within which we search for low-energy protons. These regions are defined in terms of the photon conversion length in argon (λ). At these energies, pair production dominates the interaction cross section with a mass attenuation coefficient of 0.03 cm^2/g, corresponding to a conversion length of approximately 25 cm in liquid argon. The selected angular values, α_λ, $\alpha_{2\lambda}$, and $\alpha_{3\lambda}$, are chosen to encompass the angular range at high backward angles over which an uptick in blips is observed relative to the isotropic blip population surrounding the shower vertex. The backtracking regions, along with the blip-shower variables — blip distance to the shower vertex (D) and blip angle (α), where $\alpha \in [0°, 180°]$ —

are illustrated in Figure 4.

- **Region I**: Tight (highly-collinear) backward region. $D < 3\lambda$ (75 cm) and $\alpha_{3\lambda} > 176°$.
- **Region II**: Intermediate backward region. $D < 2\lambda$ (50 cm) and $\alpha_{2\lambda} > 172°$.
- **Region III**: Loose (weakly-collinear) backward region. $D < \lambda$ (25 cm) and $\alpha_{\lambda} > 169°$.

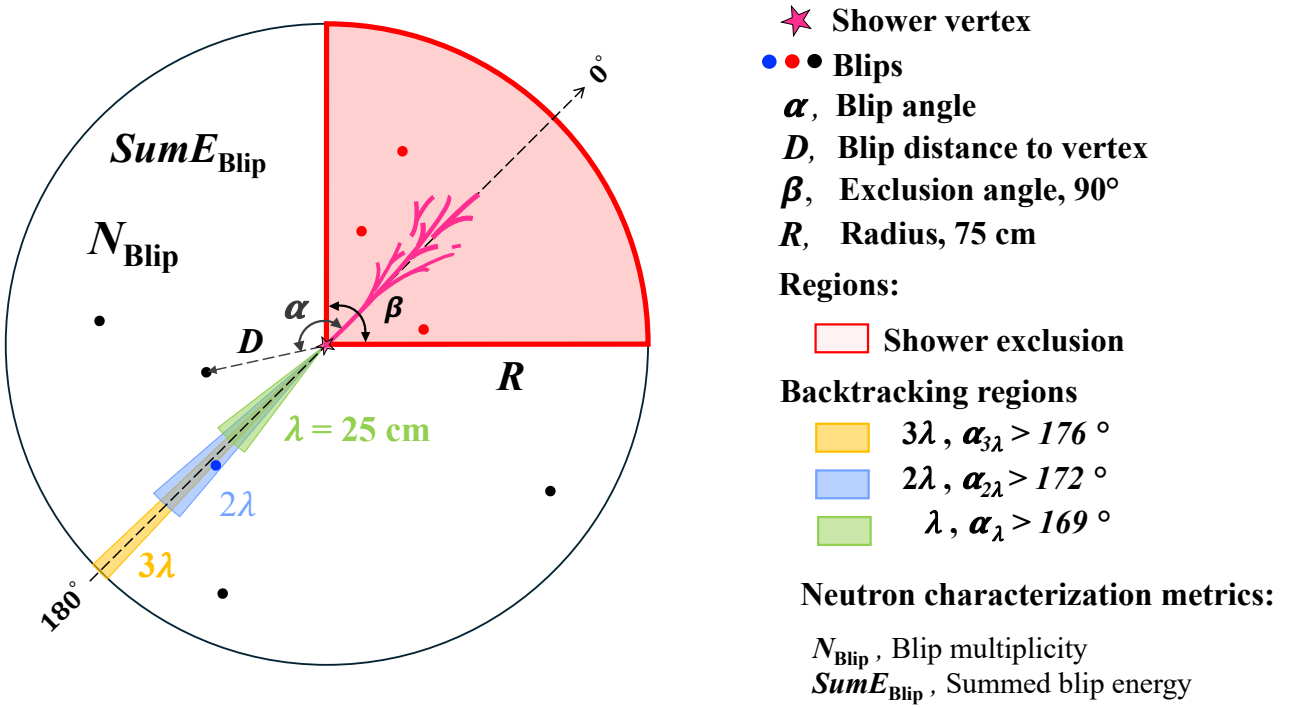

Figure 4: *Schematic of the regions defined for blip-based characterization. The shower exclusion region is shown in red. The proton backtracking "cone regions" delimited by* $(\lambda, \alpha_\lambda)$ *in green,* $(2\lambda, \alpha_{2\lambda})$ *in blue, and* $(3\lambda, \alpha_{3\lambda})$ *in yellow, where the angles are measured with respect to the shower direction. The remaining volume within the sphere is reserved for neutron characterization, quantified via the blip multiplicity* (N_{Blip}) *and the summed blip energy* ($SumE_{\text{Blip}}$) *blip metrics.*

4.1 Concepts for an enhanced 0p/Np split

For each event, blips are searched for within the backtracking regions defined above, and any blip found within these regions is counted as a proton candidate, regardless of its energy. The potential of this method for identifying sub-threshold protons to enhance $0p/Np$ separation is illustrated by the example event display in Figure 5. Additional criteria may be applied to further assess whether a given blip is proton-like, based on the electron/proton discrimination method described in Ref. [9].

The resulting distribution of reconstructed proton multiplicity after incorporating proton candidates identified through blips is shown in Figure 6. Minor changes are observed respect to Figure 2, with the total normalized $0p$ event count in the MC dataset reducing from roughly 21.2 to 19.3 expected events. A more substantial gain in proton identification might be expected if the blip-based proton identification is applied to a sample processed with lower-threshold reconstruction settings.

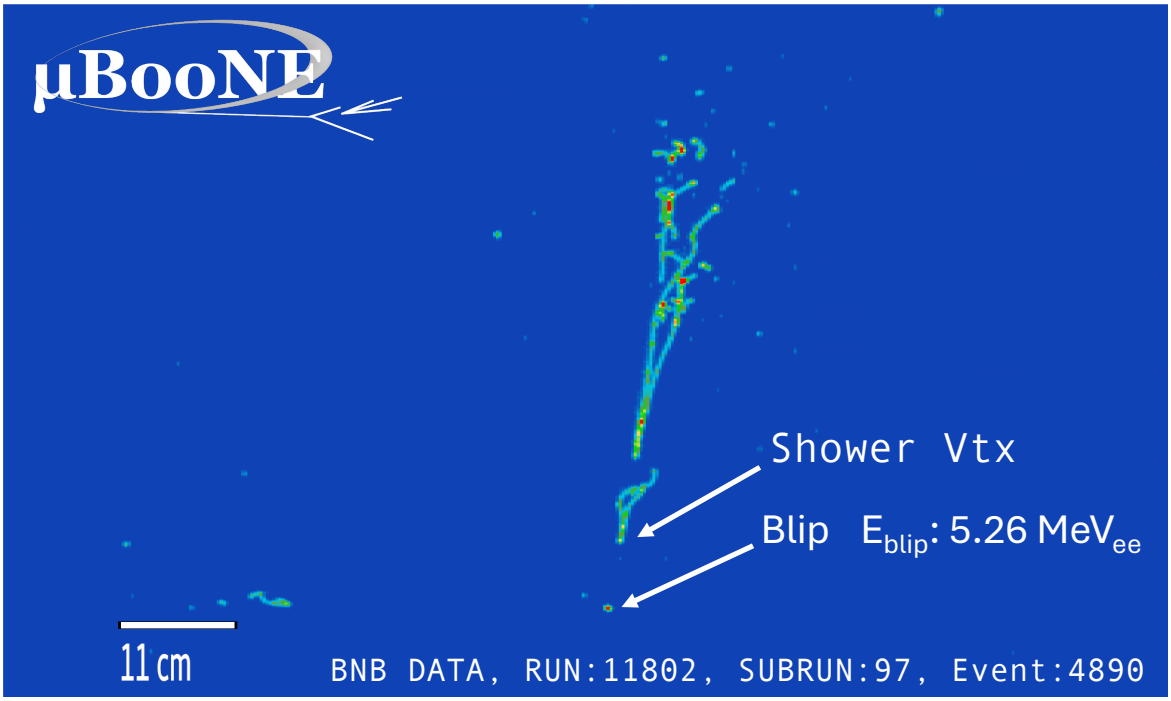

Figure 5: *Example of an inclusive single-photon data event in which no Wire-Cell reconstructed protons are found (0p). This event exhibits a backtracked blip at $\alpha = 178.7°$, located 9.5 cm from the shower vertex, which is identified as proton-like according to the proton–electron discrimination criteria of Ref. [9]. The blip has a reconstructed energy of 5.26 MeV_{ee} due to the heavier ionization density of protons, this corresponds to a true proton kinetic energy of roughly 22 MeV.*

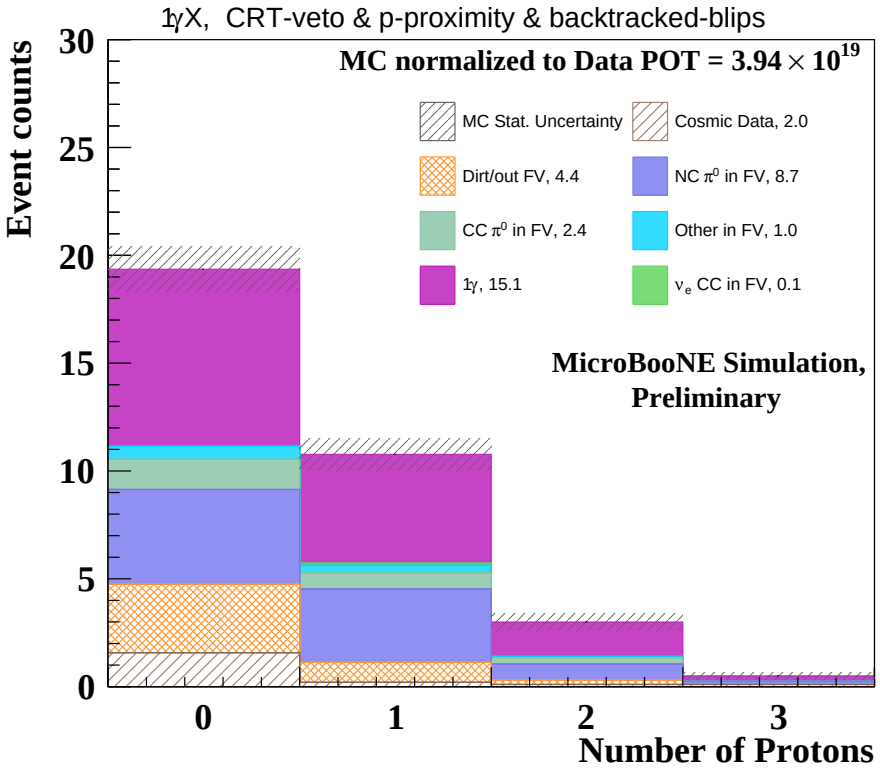

Figure 6: *The selection shown here includes the analysis improvements introduced in the present work, the CRT-veto and Wire-Cell proton proximity cuts as well as the backtracked-blips as low-energy proton candidates.*

4.2 Purity of the enhanced 0p/Np split

To get a better sense of how the demonstrated $0p/Np$ enhancement performs, we can look into the true content of signal events: true $1\gamma 0p$ and true $1\gamma Np$. The definition of the true $0p$ topology is kept consistent with that adopted in the previous analysis, thereby an event is classified as true $0p$ if it contains no final-state proton with kinetic energy exceeding 35 MeV, the threshold below which Wire-Cell proton reconstruction becomes unreliable. Ideally, blip-based change in $0p/Np$ event designations would serve to increase the purity of $0p$ and Np reconstructed samples.

Figure 7 shows these two truth-level categories in pink and red respectively. It appears that the $0p$ designation provided by Wire-Cell proton reconstruction results in relatively little contamination of the reconstructed $1\gamma Np$ and $1\gamma 0p$ samples, with the Np sample, in particular, being quite pure. As expected from the previous Section, any change in these purity levels from the addition of blip-based proton identification is modest.

Interestingly, 8.6% of 1γ events (1.83 events after scaling to the data sample size) migrate from $0p$ to Np. Of this population, for truth-labeled $0p$ (1.48 events post-scaling), 35% actually host true protons whose energies were too low to register the event as Np (requires protons with >35 MeV kinetic energy). For true-Np-labeled events migrated from the reconstructed $0p$ to $1p$ bin (0.20 events post-scaling) 75% contain true protons between 35 and 150 MeV kinetic energy. These examples highlight the specific intended benefits of blip-based proton identification for low-vertex-activity event classes.

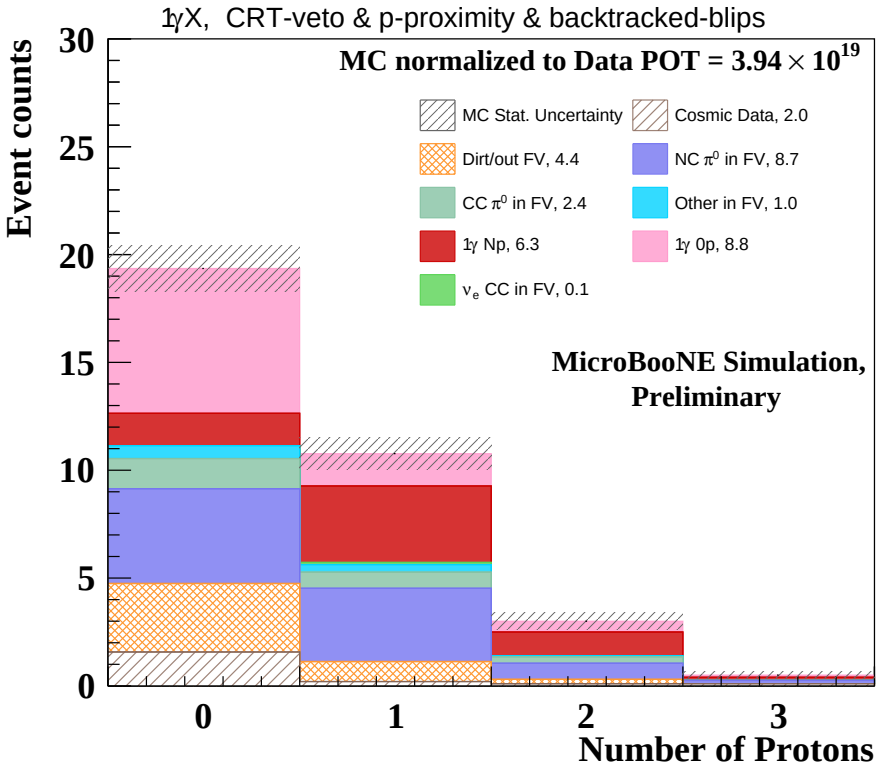

Figure 7: *Breakdown of signal events* 1γ *into true* $1\gamma 0p$ *(pink) and true* $1\gamma Np$ *(red).*

5 Neutron characterization blip metrics

Blip features are also well-suited for neutron characterization, as neutrons undergoing multiple inelastic scatterings produce a characteristic population of electron-like blips. For this purpose, two blip-based metrics are defined: blip multiplicity (N_{Blip}) and summed blip energy ($SumE_{\text{Blip}}$) within a dedicated region of interest. This region corresponds to the remaining volume after excluding both the 90° conical region along the shower direction, used to reject shower-related blips,

and the backtracking regions reserved for proton characterization, in order to prevent double-counting. Figure 4 illustrates the region of interest used for neutron presence characterization.

The underlying idea is that if neutrons are present among the final-state particles, their inelastic scatterings will induce additional blips, driving the blip multiplicity and total blip energy above the expected baseline. Consequently, events exhibiting elevated blip activity in the region of interest are more likely to contain final-state neutrons, whereas events with blip activity consistent with ambient levels are more likely to lack neutron content. One caveat is that nuclear de-excitation gamma rays may also contribute to an elevated blip count in the region of interest, and cannot be directly distinguished from neutron-induced blips under this metric alone. Notably, nuclear de-excitation gammas are not currently modeled in the simulation and their absence may shift the MC prediction for low-energy blip activity, and should be considered when interpreting any data–MC comparison in this region.

5.1 Reconstructed Nn/0n -like designations

The designation of an event as having high or low blip activity requires defining threshold values on the blip metrics N_{Blip} and $SumE_{\text{Blip}}$. For this purpose, we construct a 2D space defined by these two metrics and establish a boundary through an optimization procedure that maximizes the separation between events with elevated and nominal blip activity, based on a comparison of BNB-ν and its corresponding EXT data sample. The resulting threshold values are 2 blips and 11 MeV$_{ee}$ for N_{Blip} and $SumE_{\text{Blip}}$, respectively. Then, events satisfying $N_{\text{Blip}} > 2$ blips or $SumE_{\text{Blip}} > 11$ MeV$_{ee}$ are designated as Nn-like (high blip activity), while those failing both criteria are designated as $0n$-like (low blip activity).

Under this labeling scheme, inclusive single-photon events are split into two categories based on neutron presence. When further combined with the reconstructed proton multiplicity, four exclusive categories emerge: ***0p0n***, ***0pNn***, ***Np0n***, and ***NpNn***. These explicit designations allow a more comprehensive, quantitative characterization of the hadronic final states suggested at the beginning of this note in Section 1.1 and Figure 1. This category breakdown is now illustrated directly in Figure 8.

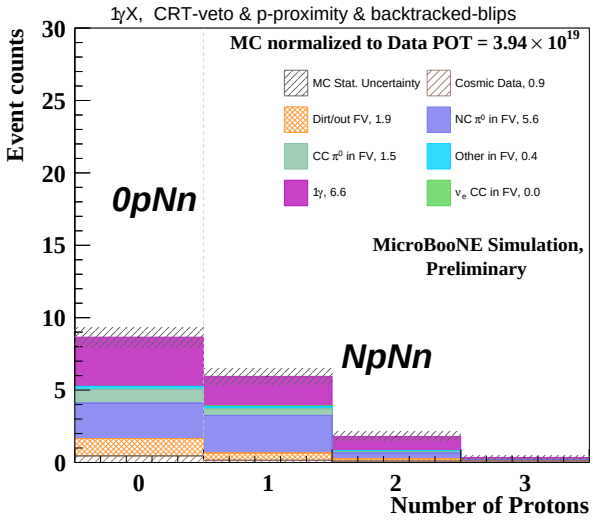

(a) Inclusive single-photon Nn-like events.

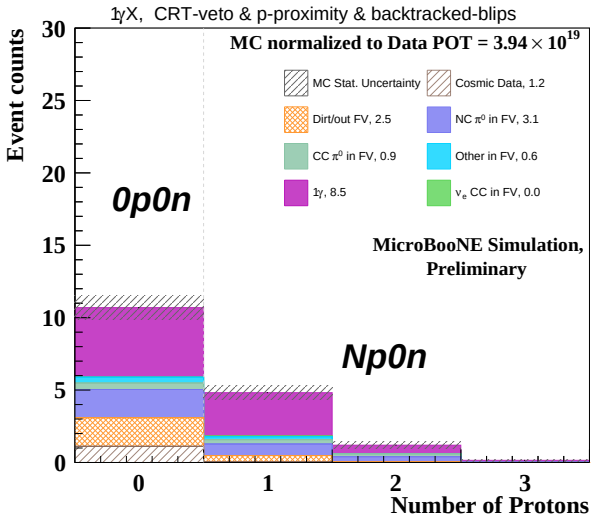

(b) Inclusive single-photon 0n-like events.

Figure 8: *Split of inclusive single-photon events into events exhibiting (a) high-blip activity (Nn-like) and (b) low-blip activity (0n-like). These plots include three analysis refinements: the CRT-veto cut, a vertex proximity requirement for Wire-Cell-reconstructed protons, and an enhanced $0p/Np$ separation leveraging backtracked blips near the shower vertex.*

The breakdown between reconstructed Nn and $0n$ categories is relatively even with 16.9 (16.8)

Nn ($0n$) for MC, respectively. Looking at the truth-level origins of the newly-defined reconstructed $0n$ category, we see that the 'signal' 1γ event category remains the predominant contributor. Interestingly, the substantial NC and CC π^0 background categories contribute a higher fraction of events in the reconstructed Nn event set than in the $0n$ event set. This observation is consistent with the presence of blips from the missing second shower of the π^0 decay in these events, where the corresponding γ-ray interaction in the TPC was not identified by the Wire-Cell shower reconstruction. It is also interesting to note that 1γ, cosmic, and out of FV (Fiducial Volume) event classes all seem similarly split between reconstructed Nn and $0n$ categories. This should perhaps not be too surprising, given that cosmic nuclear interactions and out of FV neutrino-nucleus interactions generating electromagnetic showers seem as likely as the dominant signal 1γ processes to generate widely-dispersed final-state de-excitation and neutron blips.

5.2 Truth Studies - true 0n/Nn split

In order to assess the purity of the reconstructed $0n$ and Nn designations, it is necessary to establish truth-level definitions of reconstructed $0n$ and Nn events. This task is extremely challenging for neutrons due to the nature of neutron interactions in argon: the majority of the neutronic final state's kinetic energy goes undetected, and the remainder is usually dispersed unevenly and stochastically over a large volume within and outside the active TPC. The relevant issues are well-described in Refs. [13, 14]. In the case where the neutron final-state is generated inside MicroBooNE's relatively long and narrow TPC, it has a high probability of escaping the TPC while experiencing zero or a small number of blip-generating inelastic scatters, given the long mean-free path (10s of cm) of high-energy neutrons in liquid argon. On the other hand, in the case where the neutronic final-state is generated near but outside the TPC, it will also not be unusual for it to experience a small number of blip-generating inelastic scatters inside the TPC for the same reason. A neutron with a modestly high (>10 MeV) kinetic energy is likely to undergo inelastic collisions releasing one or more secondary neutrons, resulting in a large fraction of the primary neutron energy being lost to overcoming the binding energy of these freed nucleons. Thus, we expect the boundary in kinetic energy between detectable and undetectable neutrons, as well as the linearity between neutron energy and reconstructed blip energy, to be unclear.

Unlike protons, there is no clear discriminating variable for neutrons that would allow a well-defined true $0n$ threshold to be set. Thus, based on physics arguments, we define true Nn events as those in which the total true summed final-state neutron kinetic energy is greater than 10 MeV, with the additional requirement that at least one true neutron carries kinetic energy above 5 MeV. This definition further allows the true neutronic final-state to be generated either inside or outside the TPC, in contrast to truth-level proton content definitions. Under this definition, signal events can be decomposed into neutron-present and neutron-absent categories at truth level, as shown in Figure 9, where the signal category 1γ has been split into $1\gamma 0n$ (dark blue) and $1\gamma Nn$ (orange).

Such breakdown indicates that the purity of both the reconstructed $0n$ and Nn samples are not particularly high. This should not be surprising, based on the difficulty in reconstructing neutrons with high fidelity and on the nebulous boundary between detectable and un-detectable neutrons. However, some degree of separation of truth-level categories is visible: the ratio between true Nn and $0n$ categories is 3.7 in the reconstructed Nn sample, while in the reconstructed $0n$ sample, that ratio decreases to 1.9. The primary cause for this difference is a comparatively larger fraction of events with zero true final-state neutron content being sorted into the reconstructed $0n$ category. So, while neutron identification is far from perfect, one can see that this capability does appear to generate worthwhile reductions of neutronic final-states from the single-shower sample.

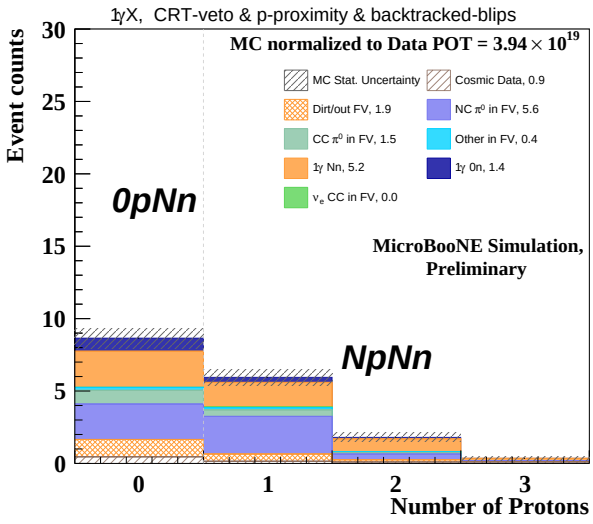

(a) Inclusive single-photon Nn-like events.

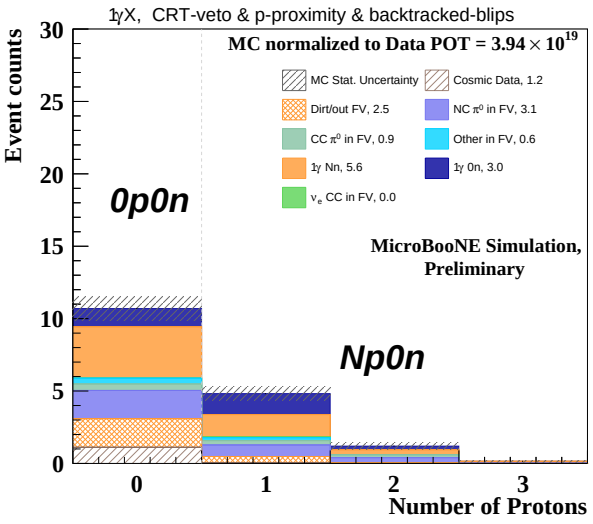

(b) Inclusive single-photon 0n-like events.

Figure 9: *Split of events into reconstructed 0n-like and reconstructed Nn-like. Signal category broken down into true* $1\gamma 0n$ *and true* $1\gamma Nn$*, dark blue and orange components, respectively.*

6 Neutral Current π^0 sideband events

The dominant background in the inclusive single-photon selection is NC π^0 events, comprising approximately 25.82% of the total selected Monte Carlo events, while the 1γ signal fraction stands at 44.81%. Summing across all truth-level categories in the analysis, NC π^0 neutrino interactions in signal (Sig) and background (Bkg) categories account for 51% of all predicted events in the single-photon selection. Given the large impact of NC π^0 production in both the signal and background categories, it is worthwhile to attempt to identify a purified sample of well-understood NC π^0 events so that rate estimates for our signal 1γ channel can be adjusted and systematically constrained by this higher-statistics, more well-understood event sample.

In particular, for our present analysis focused on hadronic final-state content near isolated single showers, it is very important to understand the hadronic makeup of these NC π^0 events, so that we can properly adjust MC predictions to sort this event type more realistically into final-state hadronic categories. As has been well-established by other prior LArTPC and accelerator neutrino experiments [12, 15–17], neutrino generator predictions of final-state hadronic and de-excitation content can be inaccurate, so direct, data-based constraints are needed to correct them and reduce associated systematic uncertainties.

The intent is to use the NC π^0-enriched sideband sample, which represents the primary background component within the 1γ signal and background regions. While these samples closely resemble those of the previously published selection criteria [1], this analysis extends the prior study by subdividing them into four event categories defined by the absence or presence of nearby reconstructed hadronic activity. This updated categorization necessitates a revised treatment of sideband constraints and systematic uncertainty propagation.

6.1 Definition of the sideband sample

In the sideband region, defined by applying the corresponding Wire-Cell inclusive single-photon sideband cuts as in the prior published analysis [1], based on inverted BDT cuts and requiring ≥ 2 showers, the signal fraction drops to 6.7%, with the NC π^0 background sub-category constituting the primary contributor at 60.4% of the total selected sample.

The full background composition after applying the selection cuts is shown in Table 1.

Table 1: *Number of inclusive single-photon and NC π^0 sideband events according to the MC, and the fraction each category contributes to the total event selection.*

	Inclusive single-photon	**NC π^0 Sideband**
(Sig) 1γ	15.1 (44.8%)	17.4 (6.7%)
(Bkg) CC π^0 in FV	2.4 (7.1%)	34.0 (13.1%)
(Bkg) Dirt/out FV	4.4 (13.1%)	26.0 (10.1%)
(Bkg) Cosmic Data	2.0 (5.9%)	15.0 (5.8%)
(Bkg) NC π^0 in FV	8.7 (25.8%)	156.2 (60.4%)
(Bkg) Other in FV	1.0 (3.0%)	6.3 (2.4%)
(Bkg) ν_e CC in FV	0.1 (0.30%)	3.8 (1.5%)
Total	33.7 (100%)	258.7 (100%)

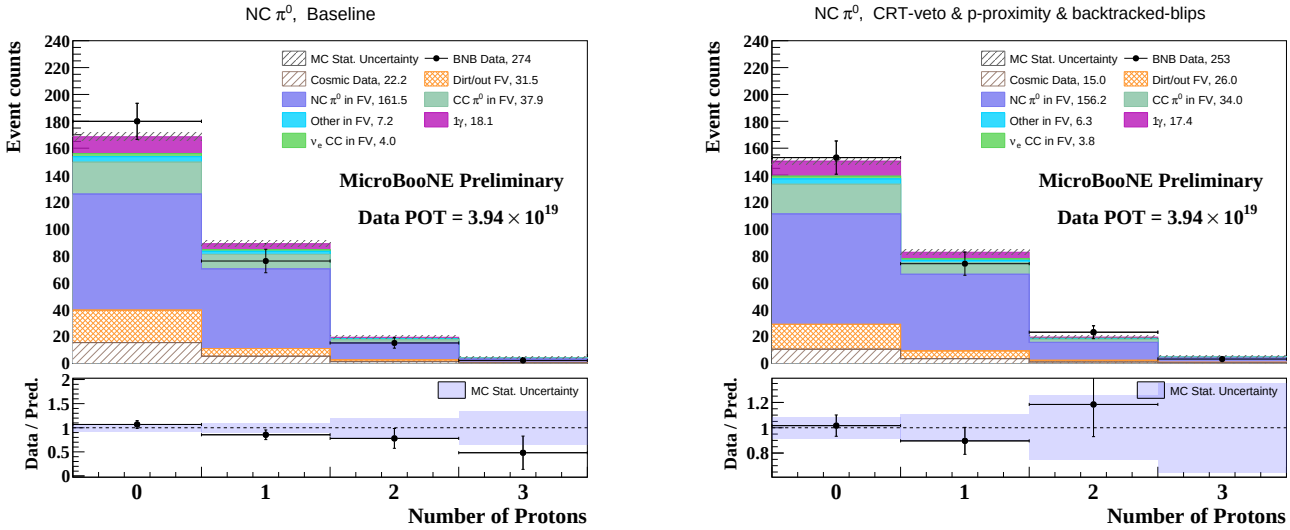

(a) *Baseline NC π^0 sideband event selection.* ***(b)*** *Updated NC π^0 sideband event selection.*

Figure 10: *Comparison of NC π^0 sideband event selections before and after the additional reconstruction and background rejection requirements. (Left) Baseline NC π^0 sideband event selection as in previous analysis. (Right) NC π^0 sideband events after applying the three additions to the present analysis: the CRT-veto cut, the vertex proximity requirement for Wire-Cell reconstructed protons, and the backtracked blip criterion for improved 0p/Np separation.*

Figure 10a shows the reconstructed proton multiplicity distribution in the NC π^0 sideband using the baseline selection cuts from the previous analysis Ref. [1], while Figure 10b shows the same distribution after applying the additional requirements introduced in the present analysis: namely, the CRT veto and the proton-to-shower proximity cut, which requires any reconstructed proton candidate to lie within 75 cm of the reconstructed shower vertex and the enhanced proton multiplicity definition, in which blips reconstructed within the backtracked regions defined relative to the shower axis are considered as proton candidates, improving the detection of low-energy sub-threshold protons and increasing the overall reconstructed proton count. Prior to the application of these additional cuts, the data-to-simulation agreement was already good across all proton multiplicity bins. The introduction of the CRT veto and the proximity requirement further improves this agreement, providing additional confidence in the modeling of the proton multiplicity in the sideband region, and consequently in the signal region.

An additional consideration for this sideband is the number of reconstructed showers. Since more than one π^0 may be present in an event, at least two showers are expected in such cases. For these scenarios, it may be necessary to restrict the analysis to the two-photon subset of the

NC π^0 sample and, when applying the blip-based techniques, to exclude the backtracked region associated with the subleading shower as well.

6.2 Split of NC π^0 sideband into reconstructed 0n/Nn

Applying the same criteria used for the inclusive single-photon sample to separate sideband events into high (Nn-like) and low ($0n$-like) blip-activity categories for the BNB MC, while masking only the leading shower from π^0 decay, yields the distributions shown in Figure 11.

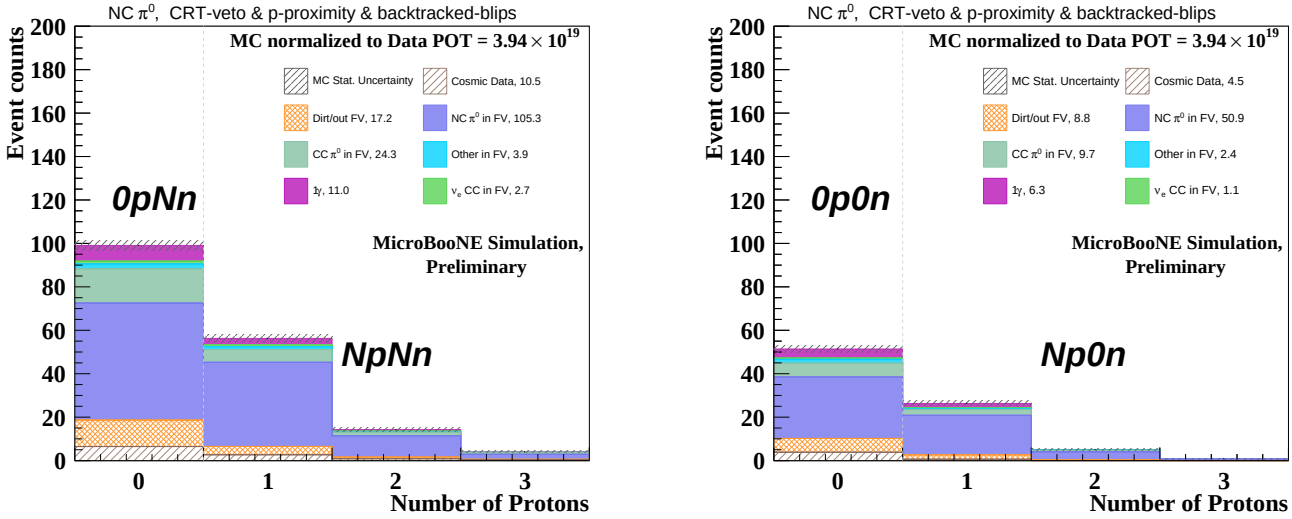

(a) *Sideband Nn-like events.* ***(b)*** *Sideband 0n-like events.*

Figure 11: *Split of sideband events into events with high (Nn-like) and low (0n-like) blip activity.*

6.2.1 NC π^0 sideband - true 0n/Nn

We adopt the same definition of true Nn and true $0n$ described in Sec. 5.2 for the sideband events. Under the present definition of true neutron content, keeping in mind the challenges associated with accurate neutron reconstruction, the selected sample is observed to contain 5.4 times more true Nn events than true $0n$ events. This enrichment is consistent with expectations. The observed $Nn/0n$ ratio a priori provides an encouraging validation on the sideband events that the blip-based selection is indeed effective at isolating events with neutron presence. Regarding the reconstructed $0n$ sample, the true $Nn/0n$ ratio is observed to be 1.8, indicating that true Nn events are almost twice as abundant as true $0n$ events in a sample intended to select events with no neutron presence. This reflects a reduced purity in this sub-dataset relative to the reconstructed Nn sample, and is not unexpected given the limitations of neutron reconstruction; neutrons that fail to produce identifiable blip activity will inevitably migrate into the reconstructed $0n$ category, constituting an irreducible source of true Nn contamination.

7 Summary

This work presents a first look at an analysis with the goal of improving the purity of the inclusive single-photon selection by incorporating new features absent in the previous analysis [1]. These include CRT-veto information to mitigate background events and blip-based techniques that provide access to hadronic activity in the final state below the standard reconstruction threshold. In particular, the identification of low-energy protons through proton-like blips enables a reclassification of reconstructed $0p$ events into reconstructed Np, while the analysis of the isotropically

distributed blip population around the shower vertex, characterized through dedicated blip metrics, provides a handle on neutron presence in the final state.

Application of blip reconstruction techniques to the existing set of selected inclusive single-shower events in Ref. [1] clearly indicates an excess of shower-external blip activity in these events compared to what is expected from ambient cosmic and radiogenic activity. This is the first time such an excess of MeV-scale activity has been reported in a sample of neutral-current neutrino-argon interactions. The result further motivates the inclusion of MeV-scale reconstruction in an enhanced search for isolated electromagnetic showers in MicroBooNE. As a result of these techniques, the inclusive single-photon events can be further classified according to their exhibited hadronic activity, specifically in terms of proton and neutron presence, into four exclusive categories: $0p0n$-, $0pNn$-, $Np0n$-, and $NpNn$-like. Similarly, the NC π^0 sideband events can be broken down into the same categories, which will prove useful when constraining each of these channels individually.

The impact of blip-based proton identification could be improved in future analysis and experiments through the use of lowered hit-finding thresholds for blip reconstruction. This will allow blips to contain lower-energy features not previously accessible in the Wire-Cell high-level reconstruction framework.

Meanwhile, we have successfully split the signal sample into sub-sets of high and low adjacent blip activity, which are colloquially interpreted as corresponding to neutron-including and neutron-excluding final state activity. This is the first time that such a blip-based separation of neutrino interaction final states has been performed on neutrino LArTPC datasets. This procedure generates approximately even breakdowns between $0n$-like and Nn-like reconstructed event categories for selected inclusive single-photon simulated events. Truth-level categorizations reveal that NC π^0 backgrounds in the 1γ-like signal are preferentially sorted into the Nn-like category, while true 1γ, out of FV, and cosmic subsets slightly prefer the $0n$-like categorization. While the true hadronic purity of Nn-like and $0n$-like reconstructed samples are low, as should be expected for this sample of TPC-edge-preferring events in the narrow MicroBooNE TPC, we can clearly see a higher proportion of true $0n$ events in the reconstructed $0n$ category.

References

[1] P. Abratenko et al. (MicroBooNE Collaboration). Inclusive Search for Anomalous Single-Photon Production in MicroBooNE. *Phys. Rev. Lett.*, 136:181806, 2026.

[2] A. A. Aguilar-Arevalo et al. (MiniBooNE Collaboration). Updated MiniBooNE neutrino oscillation results with increased data and new background studies. *Phys. Rev. D*, 103:052002, 2021.

[3] P. Abratenko et al. (MicroBooNE Collaboration). Search for an Anomalous Production of Charged-Current ν_e Interactions without Visible Pions across Multiple Kinematic Observables in MicroBooNE. *Phys. Rev. Lett.*, 135:081802, 2025.

[4] The MicroBooNE Collaboration. Search for light sterile neutrinos with two neutrino beams at MicroBooNE. *Nature*, 648(8092):64–69, 2025.

[5] P. Abratenko et al. (MicroBooNE Collaboration). Enhanced search for neutral current Δ radiative single-photon production in MicroBooNE. *Phys. Rev. D*, 112:L091101, 2025.

[6] P. Abratenko et al. (MicroBooNE Collaboration). First Search for Neutral Current Coherent Single-Photon Production in MicroBooNE, 2025, arXiv:2502.06091 [hep-ex].

[7] Abdullahi et al. (MicroBooNE Collaboration). First Search for Dark Sector e^+e^- Explanations of the MiniBooNE Anomaly at MicroBooNE. *Phys. Rev. Lett.*, 136:121804, 2026.

[8] P. Abratenko et al. (MicroBooNE Collaboration). Measurement of ambient radon progeny decay rates and energy spectra in liquid argon using the MicroBooNE detector. *Phys. Rev. D*, 109:052007, 2024.

[9] P. Abratenko et al. (MicroBooNE Collaboration). Demonstration of new MeV-scale capabilities in large neutrino LArTPCs using ambient radiogenic and cosmogenic activity in MicroBooNE. *Phys. Rev. D*, 111:032005, 2025.

[10] P. Abratenko et al. (MicroBooNE Collaboration). Characterizing the energy resolution of the MicroBooNE LArTPC at the MeV scale using monoenergetic features of ^{208}Tl decays. 2026, arXiv:2605.30709 [physics.ins-det].

[11] P. Abratenko (MicroBooNE Collaboration). Observation of radon mitigation in MicroBooNE by a liquid argon filtration system. *J. Instrum.*, 17:P11022, 2022.

[12] R. Acciarri et al. (ArgoNeuT Collaboration). Demonstration of MeV-scale physics in liquid argon time projection chambers using ArgoNeuT. *Phys. Rev. D*, 99:012002, 2019.

[13] W. Castiglioni, W. Foreman, I. Lepetic, B. R. Littlejohn, M. Malaker, and A. Mastbaum. Benefits of MeV-scale reconstruction capabilities in large liquid argon time projection chambers. *Phys. Rev. D*, 102:092010, 2020.

[14] S Andringa et al. Low-energy physics in neutrino LArTPCs. *J. Phys. G*, 50(3):033001, 2023.

[15] M. Elkins et al. (MINERvA Collaboration). Neutron measurements from antineutrino hydrocarbon reactions. *Phys. Rev. D*, 100:052002, 2019.

[16] A. Olivier et al. (MINERvA Collaboration). Measurement of the multineutron $\bar{\nu}_\mu$ charged current differential cross section at low available energy on hydrocarbon. *Phys. Rev. D*, 108:112010, 2023.

[17] P. Abratenko et al. (MicroBooNE Collaboration). Inclusive cross section measurements in final states with and without protons for charged-current ν_μ-Ar scattering in MicroBooNE. *Phys. Rev. D*, 110:013006, 2024.